Available online at www.sciencedirect.com
SCIENCE DIRECT®

Journal of the European Ceramic Society 24 (2004) 2103–2111

www.elsevier.com/locate/jeurceramsoc

# Surface and bulk crystallization in $Nd_2O_3$–$Al_2O_3$–$SiO_2$–$TiO_2$ glasses

Hyungsun Kim*, Woohyung Choi

*Department of Material Science and Metallurgical Engineering, Sunchon National University, Sunchon 540-742, South Korea*

Received 26 January 2003; received in revised form 16 May 2003; accepted 25 May 2003

**Abstract**

Neodymium aluminosilicate ($Nd_2O_3$–$Al_2O_3$–$SiO_2$; NdAS) glasses have been investigated for the effect of concentration of $TiO_2$ on the crystallization mechanism and for the effect of surface condition on crystal growth. NdAS glasses with 0–10 wt.% $TiO_2$ were heat-treated for nucleation and crystal growth and were examined for phase separation and morphology of surface crystals as well as for crystal growth rate. All the glasses exhibit surface crystallization, however, the glass having 8 wt.% $TiO_2$ also exhibits internal crystallization after a two-stage heat treatment. Surface crystallization was dependent on the condition of the glass surface and the amount of $TiO_2$. The crystal growth on the cut surface was faster than on the fractured surface and the growth rate in surface increased with increasing $TiO_2$. The phase separation found in NdAS glasses containing above 8 wt.% $TiO_2$, was confirmed to be an important factor controlling the internal crystallization process in $Nd_2O_3$–$Al_2O_3$–$SiO_2$–$TiO_2$ glasses.

*Keywords:* Crystallization; Glass; $Nd_2O_3$–$Al_2O_3$–$SiO_2$; Nucleation; Surfaces; $TiO_2$

## 1. Introduction

Because of the unique optical and magnetic behavior of rare-earth oxides, rare-earth glass systems have recently been studied for use in lasers, sensors, radiation resistant glasses and other applications. Since late 1980, much of the research on rare-earth glass systems has been devoted to evaluation of the properties of glasses.[1,2] Before that time, there were many works on silicate glass systems doped with rare-earth ions, containing less than a few wt.%. Since then, however, research has had a new paradigm in which rare-earth oxide was increased to up to 20 mol% of silicate systems in order to find some application of the glasses.[3,4] In spite of many works on rare-earth oxides silicate glasses, no research was found on the comparable glass–ceramics. These would have several advantages in terms of special properties such as mechanical, thermal, optical and magnetic properties as compared with the glasses. The author has carried out basic research on surface crystallization of the $Nd_2O_3$–$Al_2O_3$–$SiO_2$ (NdAS) glasses,[5,6] because the NdAS system has very similar thermal, electrical and physical properties with other rare-earth aluminosilicate glasses.[1–4]

In this study, it was decided to study the effect of $TiO_2$ on the surface and internal crystallization mechanism and the effect of glass surface condition on the crystal growth in order to reveal the crystallization phenomena of neodymium aluminosilicate glasses. The result would be applied to also other rare-earth aluminosilicate glasses and to high temperature sealing glass–ceramics in electrical equipment.

## 2. Experimental procedure

Glasses were prepared by melting a $15Nd_2O_3$–$20Al_2O_3$–$65SiO_2$ (mol%) and $TiO_2$ (0, 4, 6, 8,10 wt.%) in a Pt–Rh (20%) crucible at 1550 °C for 6 h. The melts were poured into a graphite mold, followed by annealing at $T_g$ + 10 °C for 1 h. Samples were then heat-treated for nucleation at 890 °C for 1–4 h and for crystal growth at 1000–1200 °C for 1–4h. In the differential thermal analysis (DTA) measurement, two different samples were used to measure the effect of surface and internal crystallization: one was powder type (frit (<38 μm), as-quenched glass) and the other bulk states prepared by heating at 890 °C for 30–600 min after melting

---

* Corresponding author. Tel.: +82-61-750-3555; fax: +82-61-750-3550.

*E-mail address:* hskim@sunchon.ac.kr (H. Kim).

0955-2219/03/$ - see front matter © 2003 Elsevier Ltd. All rights reserved.
doi:10.1016/S0955-2219(03)00357-1

the frit at 1500 °C and cooling the bulk (pre-nucleation treatment).

The microstructure of the glass-ceramic was examined for phase separation and morphology of surface and internal crystals by scanning electron microscopy (SEM, Hitachi Co., Japan, S-4500N). Crystal phases were determined using X-ray diffraction (XRD, Shimatsu XD-1, Japan) from polished glass–ceramics (bulk) and powder under the following conditions: Cu$K_\alpha$ (Ni filter), 30 kV-20 mA, scanning speed 0.5°/min, slits of incidence angle (DS) 1.0°, detection angle (SS) 1.0°, and slit spacing (RS) 0.3 mm. To investigate the crystal phase formation in the volume of glass, the surface layer was removed by grinding after the heat treatment of the glass. Energy dispersive X-ray spectroscopy (EDS) and field emission scanning electron microscope (FESEM, EDAX-Oxford ISIS 300, 10KV) were used to analyze the chemical composition of the residual glass and the crystalline phase of the glass–ceramic, which allows a spatial resolution on the sample close to a few nm. Fracture surfaces of the samples (glasses heat treated) were etched in 1% HF solution for 40 s and were coated with carbon in vacuum to observe the morphology of phase separation. The thermal events of the glass powders (−38 μm) and bulk samples were studied by differential thermal analysis (TA Instruments 2910, USA) at 10 K/min in air. Vickers hardness was measured using a microhardness tester (MVK-E3, Mitutoyo, Japan) with a pyramid-shaped diamond indenter (a load of 500 g for 15 s) and the thermal expansion coefficient was measured for annealed glass samples (heated in air at 5 K/min) with a dilatometer (TA Instruments 4100, USA).

## 3. Results

### 3.1. Thermal analysis

The glass transformation temperatures ($T_g$) of glasses were in the range of 847–894 °C and the exothermic crystallization ($T_p$) at 1016–1098 °C, which depended on the content of $TiO_2$ in the glass. $T_g$ and $T_p$ decreased with increasing $TiO_2$ content, as shown in Fig. 1. At and above 8 wt.% of $TiO_2$, $T_g$, $T_x$ (the onset temperature of crystallization) and $T_p$ are notably affected by the change of the $TiO_2$ composition in NdAS. When a bulk glass was used for DTA measurements, $T_p$ was approximately 30 °C higher than that of the powder sample. It should be noted that NdAS glass not containing $TiO_2$ did not show any indication of exothermic reaction during the thermal event although glass powder was used (Fig. 1). The glass transformation temperature of glass (NdAS) is in the range of 860–900 °C as reported elsewhere (about 868 and 880 °C for $20Nd_2O_3$–$20Al_2O_3$–$60SiO_2$ and $18Nd_2O_3$–$31Al_2O_3$–$50SiO_2$ (mol%).[3,7] From Fig. 1, when the $T_g$ of NdAST are considered with that of NdAS, it seems that $TiO_2$ acts as a network modifier in these glasses as suggested by others.[8]

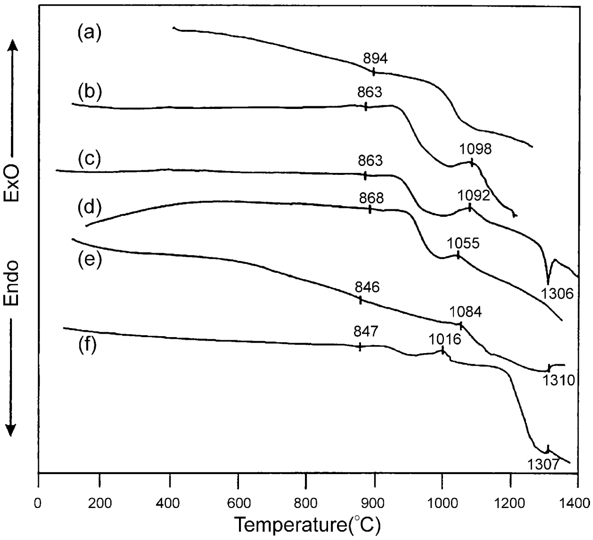

Fig. 1. DTA results of glasses (powder: <38 μm, bulk) with different content of $TiO_2$. Powder: (a) without $TiO_2$, (b) 4 wt.%, (c) 6 wt.%, (d) 8 wt.%, (f) 10 wt.% Bulk: (e) 8 wt.%.

DTA result suggested that NdAS glasses were not devitrified at all by surface or internal crystallization, while $Nd_2O_3$–$Al_2O_3$–$SiO_2$–$TiO_2$ (NdAST) glasses crystallized by only surface crystallization as a dominant mechanism in crystallization.[5,6] To induce internal (bulk, volume) crystallization, a two-stage heat treatment was carried out in NdAST glasses. A bulk glass (NdAST 8 wt.%) was nucleated at 890 °C for 0.5, 2, 4 and 10 h then heated in DTA at a heating rate of 10 K/min (see Fig. 2). The DTA curve from the bulk glasses shows a strong exothermic peak ($T_p$) at $T_p = 1118$–$1170$ °C, corresponding to the formation of internal crystals from nuclei. After 2 h heat treatment, two exo-

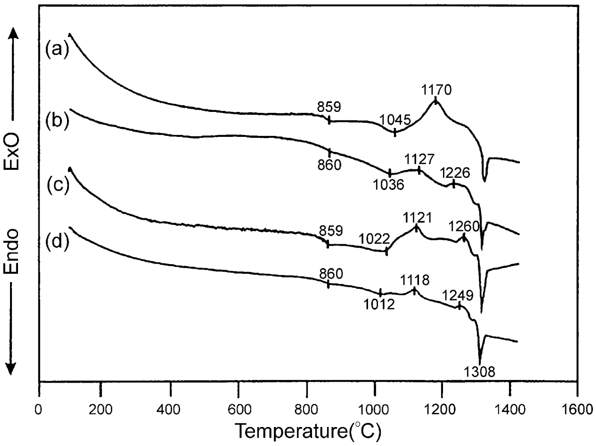

Fig. 2. DTA results for bulk NdAST–8 wt.% $TiO_2$ glasses heat treated at 890 °C for different times (Conditions in DTA test: heating rate 10 K/min in air using 60 mg bulk containing 8 wt.% $TiO_2$). (a) 30 min, (b) 120 min, (c) 240 min, (d) 600 min.

thermic peaks ($T_{p1}$ = 1118–1127 °C, $T_{p2}$ = 1226–1260 °C) were observed for the bulk glass samples. With pre-nucleation treatment, the crystallization of glass occurred at higher temperature compared to a process without a nucleation treatment at 890 °C. There are no significant differences in $T_p$ after 120 min of heat treatment in the glass (8 wt.%$TiO_2$) (Fig. 2). The $T_g$ of bulk samples heat-treated at 890 °C did not change at all during non-isothermal treatment, even though they were held for 600 min, which means that the glasses show the same relaxation phenomenon until the crystallization starts.

### 3.2. Crystallization

From the result of Fig. 1d, a DTA scan of a powder sample (8 wt.%TiO2) was interrupted at 1060 °C and, after quenching the sample, it was analyzed by XRD. An unknown crystal phase formed from the fine particle size glass during heating (Fig. 3a). However, in the case of a bulk sample which was not nucleated, it was not internally crystallized and showed a very thin surface crystalline layer. On the other hand, after nucleation at 890 °C for 1 h, quenched bulk samples at 1150 and 1270 °C showed internal crystallization. XRD peaks suggest no different crystalline phases in spite of two exothermic peaks from the DTA scans (Fig. 3b and c): a bulk sample interrupted at 1270 °C showed a fully crystalline phase compared with other samples interrupted a lower temperature, 1150 °C, which contained some glass phase (residual glass) as well as a crystalline.

A crystalline phase started to form from the glass surface (NdAST-10 wt.%) after a single heat treatment at 1100 °C for 1 h (Fig. 4a) and the Ti and Nd constituents were observed to be rich in the crystals (Fig. 4d) compared to the glass and residual glass region (Fig. 4b and c). Surface crystallization in the NdAST system was dependent on the condition of the glass surface (the number of nucleation sites) and the amount of $TiO_2$ in the glass as shown in Table 1. Surface crystals appear after a single heat treatment at 1100 °C for 8 h in samples with at least 8 wt.% of $TiO_2$ in samples with a rough cut surface formed by a diamond blade, and

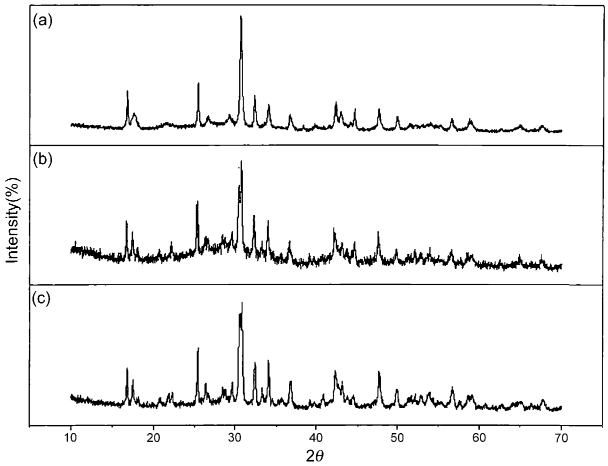

Fig. 3. XRD patterns (a) for glass powder (8 wt.%): non-isothermal heat treated from room temperature to 1060 °C, which is above $T_p$. (b) for glass bulk (8 wt.%): after nucleation at 890 °C for 1 h, non-isothermal heat treated up to 1150 °C (c) for glass bulk (8 wt.%): after nucleation at 890 °C for 1 h, non-isothermal heat treated up to 1270 °C.

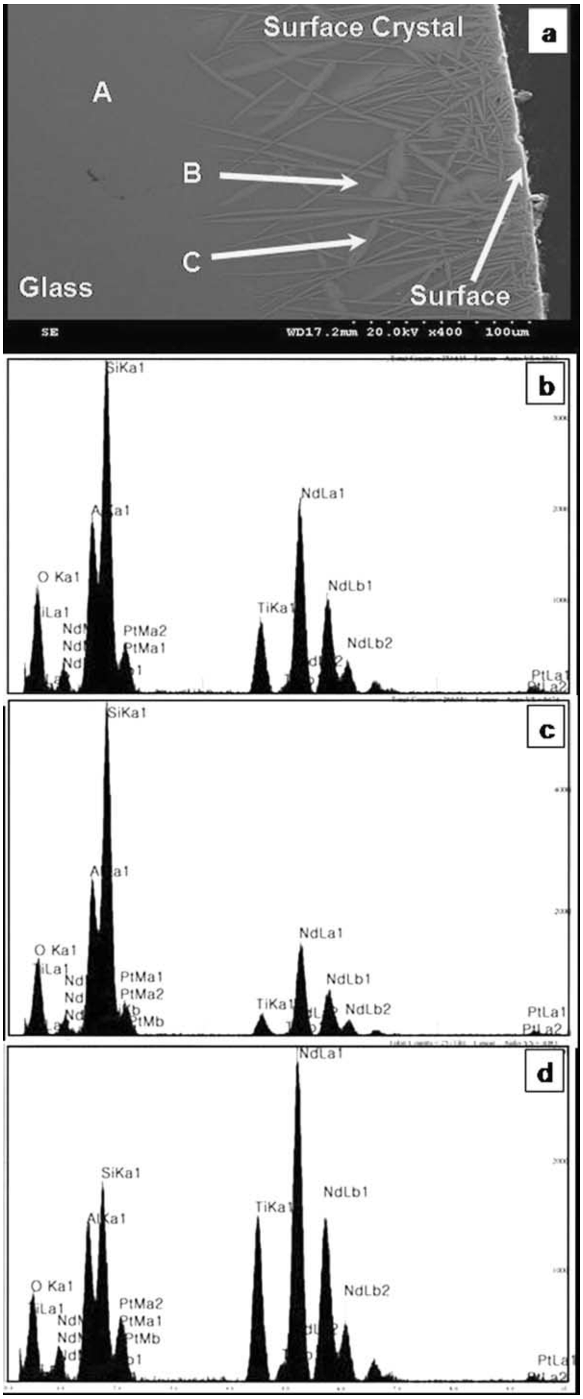

Fig. 4. SEM photograph (a) of surface crystallization (at 1100 °C for 1 h) and (b), (c) and (d), EDS result on glass [A in Fig. 1(a)], residual glass [B in Fig. 1(a)] and crystal phase [C in Fig. 1(a)], respectively.

Table 1
The result of surface crystal growth on the condition of glass surfaces and $TiO_2$ content

| | Temperature (°C) | | | | | | | | | | | |
|---|---|---|---|---|---|---|---|---|---|---|---|---|
| | 1000 | | | | 1050 | | | | 1100 | | | |
| $TiO_2$ (wt.%) | 4 | 6 | 8 | 10 | 4 | 6 | 8 | 10 | 4 | 6 | 8 | 10 |
| *Glass surface* | | | | | | | | | | | | |
| cut[a] | N | N | N | Y | N | N | N | Y | N | N | Y | Y |
| fractured | N | N | N | N | N | N | N | N | N | N | N | Y |
| cast | N | N | N | N | N | N | N | N | N | N | N | Y |

Y, surface crystal growth, N, no crystal growth.
[a] Cut by a diamond blade.

above 10 wt.% in samples with a flat fractured or cast surface. The two different surfaces (cut and fractured) gave different crystal growth rates at 1050 °C (Fig. 5): the crystal growth on the cut surface (11.5 μm/min) was faster than on the fractured surface (2.8 μm/min) in the same material (NdAST-10). With increasing $TiO_2$ content, the surface growth rate increased: 8.0±0.2 and 13.4±0.2 μm/min for 4 and 8 wt.% $TiO_2$, respectively (for polished glasses at 1150 °C).

Surface and internal crystals simultaneously were observed only in samples with 8 and 10 wt.% $TiO_2$ (heat treated at 890 °C for 4 h and at 1100 °C for 1 h for nucleation and crystal growth, respectively). Typical microstructures of crystallization are shown in Fig. 6 for different nucleation and crystal growth conditions. For internal crystallization, two conditions were required: a two-stage heat treatment and a minimum concentration of $TiO_2$ . Despite a two-stage heat treatment process to induce internal crystallization, a glass containing 6 wt.% $TiO_2$ gave predominantly surface crystallization, whereas glass containing 8 wt.% $TiO_2$ showed internal crystallization. Fig. 6 shows clearly the effect of the heat treatment time in nucleation (Fig. 6a and b) and of the heat treatment time in crystal growth during the two-stage heat treatment. With increasing time for nucleation (from 4 to 8 h at 890 °C) under the same condition for crystal growth, the number of nuclei increased and resulted in many more small crystals. On the other hand, the longer heat treatment time in crystal growth stage (from 5 to 10 min at 1150 °C) produced larger crystals from the fixed number of nuclei (Fig. 6c and d).

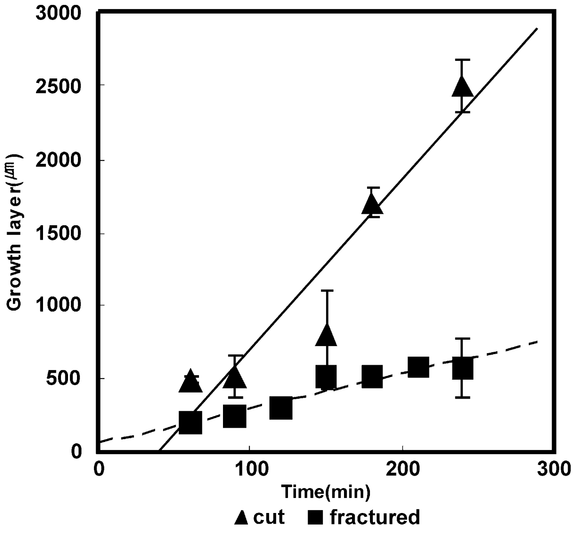

Fig. 5. Surface crystal growth rates of glasses (NdAS–10 wt.% $TiO_2$) for different surface conditions (at 1050 °C).

The surface and internal crystals, which were found to have the formula, $Nd_{4.8}Si_{7.8}Al_{3.7}Ti_{1.8}O_{32}$ by EPMA, are not found in the JCPDS–ICDD file.[9] These crystals were found to be a triclinic structure with lattice parameters, $a=10.5001$, $b=16.489$, $c=6.7389$ Å and $\alpha=92.8^\circ$, $\beta=91.2^\circ$, $\gamma=75.5^\circ$ $V=1128.2$ Å$^3$ (Table 2), where the Miller indices were calculated using CRYSFIRE program.[10] XRD patterns of glass–ceramics showed increasing crystallinity as crystal growth time increased from 2 to 8 h under the same conditions of nucleation heat treatment (Fig. 7).

Internal crystallization of NdAST glass occurred only after nucleation treatment to induce phase separation producing a number of droplets distributed throughout the bulk glass (Fig. 8). The internal crystallization mechanism consists of a droplet formation phase, a droplet crystallization phase, and completion of crystallization. When the concentration of $TiO_2$ exceeds 8

Table 2
Miller indices and relative intensity of unknown crystal phase in NdAST-8 investigated by powder diffraction method

| 2θ | I/Io | H k l |
|---|---|---|
| 12.250 | 21 | 1 2 0 |
| 16.350 | 80 | 0−2 1 |
| 17.532 | 50 | −1 1 1 |
| 20.823 | 20 | −1−3 1 |
| 22.271 | 30 | 0 4 0 |
| 25.395 | 60 | 0−4 1 |
| 26.358 | 21 | 2−2 1 |
| 28.602 | 25 | 2 4 1 |
| 29.588 | 30 | 3 0 1 |
| 30.435 | 80 | 0−5 1 |
| 30.757 | 100 | 0−3 2 |
| 32.341 | 50 | −3−4 1 |
| 33.216 | 20 | −2−3 2 |
| 33.995 | 50 | −3 2 1 |
| 35.716 | 17 | 0−6 1 |
| 36.745 | 30 | −3−2 2 |
| 39.534 | 10 | −3−4 2 |
| 40.811 | 20 | 0 1 3 |
| 42.269 | 26 | 0 2 3 |
| 47.673 | 20 | −3−2 3 |
| 49.816 | 20 | −3−4 3 |
| 52.870 | 10 | 4 5 1 |
| 53.370 | 10 | −6−3 1 |
| 56.737 | 10 | −4−8 2 |
| 64.09 | 20 | 5 8 2 |

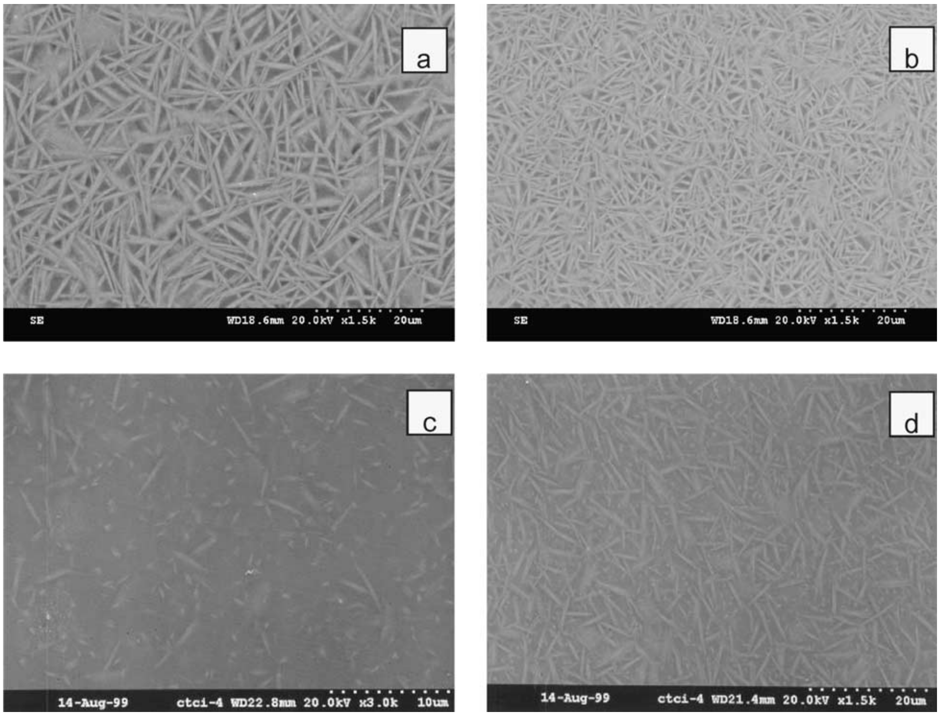

Fig. 6. SEM photographs of internal crystals resulting from different nucleation (a, b) and crystallization growth (c, d) conditions (NdAS–10 wt.% $TiO_2$): nucleation at 890 °C for 4 h (a) and 8 h (b) with crystal growth at 1150 °C for 1 h; after nucleation at 890 °C for 4 h, crystal growth at 1150 °C for 5 min (c ) and 10 min (d).

wt.%, the glass exhibits internal crystal growth after a two-stage heat treatment (Fig. 6).

The optimum nucleation temperature of the glass containing 8 wt.% $TiO_2$, was obtained using different indirect methods from thermal analysis rather than experimental methods that count nucleation rate as a function of temperature (Table 3) and was found to be in the range of 850–900 °C. As shown in Fig. 8a, large droplets are randomly distributed in the glass matrix and are larger than 10 μm in diameter. Under higher magnification, a multiple phase separation was observed, with $TiO_2$ rich small droplets ($<0.1$ μm) in a $Nd_2O_3$ rich large droplet ($>10$ μm) (Fig. 8b). After heat treatment at the first stage (a nucleation step), the glass was a milky blue color, with uniform multiple phase separation, into $Nd_2O_3$ rich isolated droplets and a $TiO_2$ rich region (Table 4). Further heat treatment (crystal growth step) induced a fine crystal microstructure of needle type as an internal crystallization (Fig. 6)

Table 5 gives the coefficient of thermal expansion (CTE) and Vickers hardness (Hv) of the NdAST glasses studied. There is good agreement between the CTE and Hv values reported,[3,14] previously and those of the NdAST glasses in the present work, although NdAST glasses include a small amount of $TiO_2$. The CTE and Hv increase with increasing crystallinity of the glass–ceramic produced by long holding times for crystal growth (Table 5). The slight increase of CTE is attributed to the change of glass to the glass–ceramic, forming a crystalline phase which has a higher CTE than that of glass. The increased heat treatment for crystal growth produced slightly increased CTE and hardness of glass–ceramic due to high crystallization, forming micropores in the matrix.

Table 3
The optimum nucleation temperature ($T_n$) of NdAST (8 wt.%$TiO_2$) predicted by several methods[a]

| Prediction methods | Data resources | Optimum nucleation temperature (°C) |
|---|---|---|
| $T_n = T_g + 2/3\ (T_d - T_g)$ | Dilatometer[11] | 887 |
| $T_f < T_n < T_f + 50$ | DTA[12] | $852 < T_n < 902$ |
| $T_g < T_n < T_g + 30$ | DTA[13] | $863 < T_n < 893$ |

[a] Where $T_d$ and $T_g$ mean the dilatometric softening point (by dilatometer) and the glass transition temperature (by DTA), respectively. $T_f$ representss the endothermic peak temperature in DTA curves $T_n$; the temperature of maximum nucleation rate.

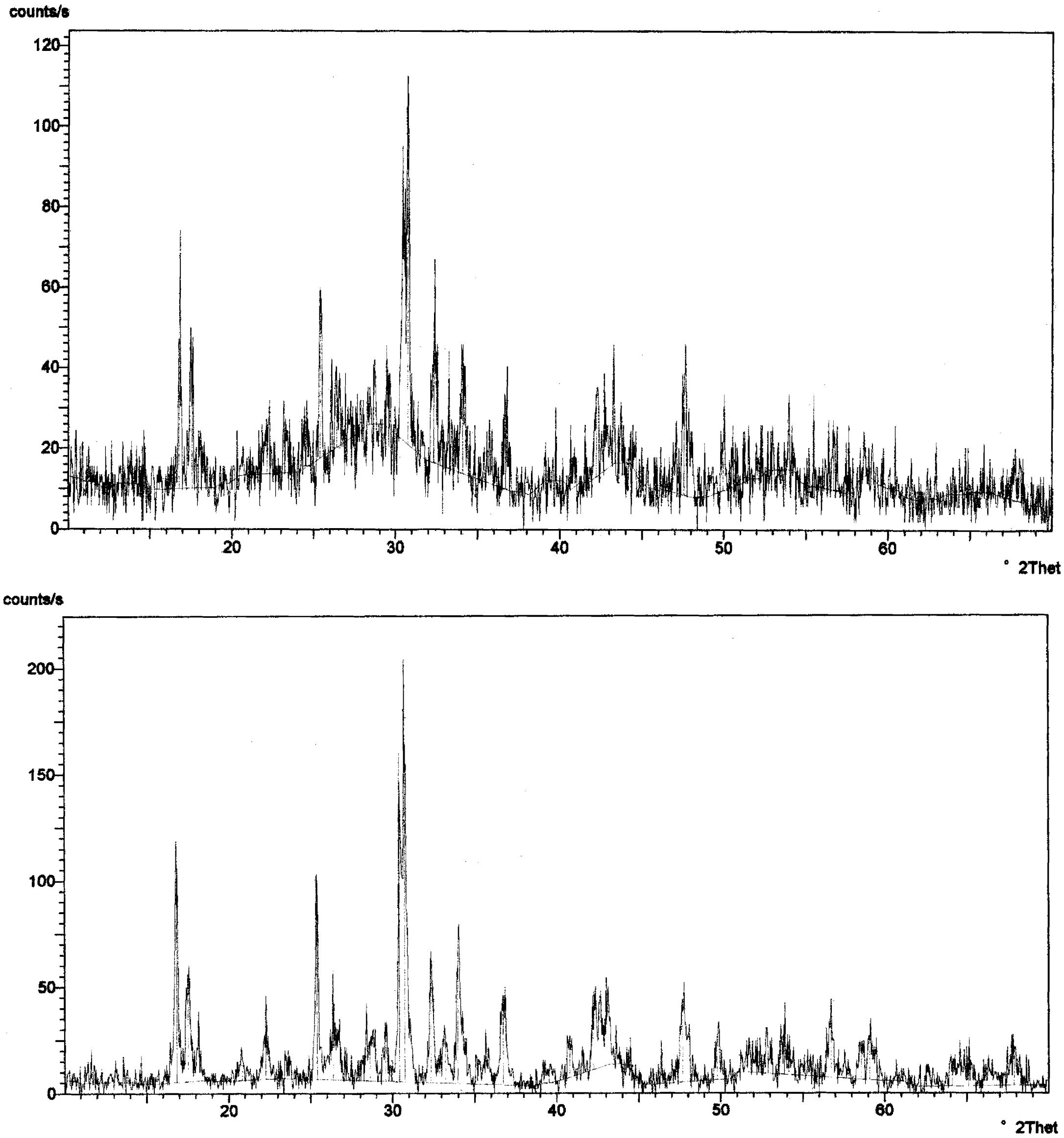

Fig. 7. XRD spectra showing the crystallization of glass (8 wt.% $TiO_2$) heat-treated at 1100 °C for 1 h (a) and for 8 h (b) after the samples were nucleated at 890 °C for 4 h.

Table 4
Chemical composition (in wt.%) of each area in Figs 4, 6 and 8

| Components | Glass | Phase separated glass | | Internal crystals | |
|---|---|---|---|---|---|
| | Matrix | Large droplet[a] | Small droplet | Crystal | Residual glass |
| $Nd_2O_3$ | 57.8 | 70.5 | 51.7 | 48.1 | 39.3 |
| $Al_2O_3$ | 9.2 | 6.8 | 11.7 | 12.9 | 19.7 |
| $SiO_2$ | 25.1 | 16.0 | 27.8 | 27.2 | 31.7 |
| $TiO_2$ | 7.9 | 6.7 | 8.8 | 11.8 | 9.3 |

[a] Using HF solution (an etchant).

Table 5
Coefficient thermal expansion (CTE) and Vickers hardness of glass/glass–ceramics

| Properties | 8 wt.% $TiO_2$–NdAS | | | |
|---|---|---|---|---|
| | Glass | Glass–ceramics | | |
| | No nucleation N-8 h | N-8 h/C-1 h[a] | N-8 h/C-4 h | N-8 h/C-8 h |
| $\alpha(10^{-6}/^{\circ}C)$[b] | 5.2 (5.55)[c] | 5.6 | 6.3 | 6.2 |
| Hv(500g) GPa | 6.92±0.04 (6.7)[d] | 8.00±0.04 | 8.53±0.06 | 8.33±0.09 |

[a] Nucleation (*N*) at 890 °C for 8 h and crystal growth (C) at 1100 °C for 1–8 h.

[b] $100 < \alpha < 300$ °C.

[c] For 15 $Nd_2O_3$–$20Al_2O_3$–$65SiO_2$ (mol%) ($200^{\circ} < \alpha < 500$ °C).[3]

[d] For 20 $Nd_2O_3$–$20Al_2O_3$–$60SiO_2$ (mol%) (load of 50 g).[14]

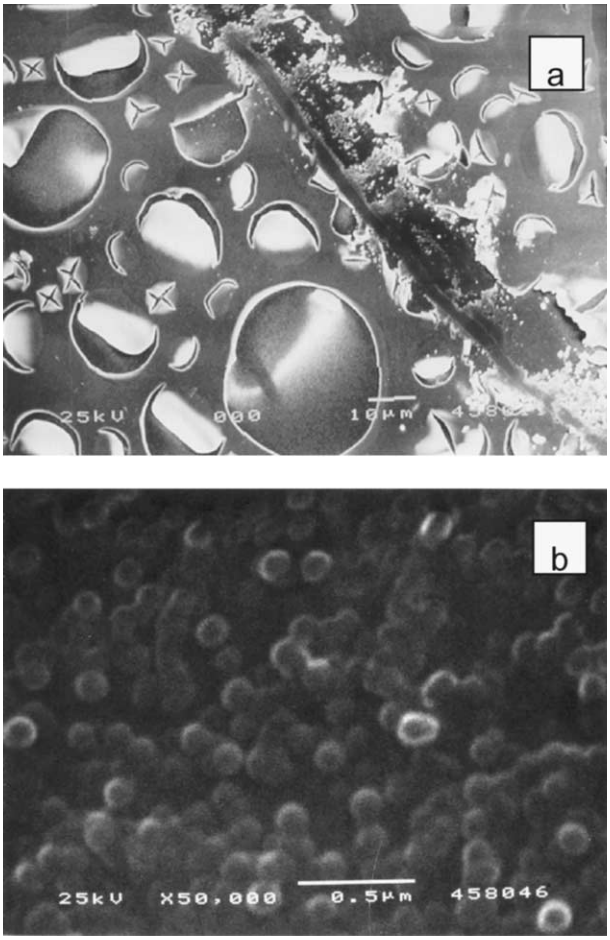

Fig. 8. SEM micrographs showing phase separation of NdAST heat treated at 890 °C for 4 h: (a) fractured glass surface with a number of droplets and (b) the droplet phase (cluster) of one of large droplets after HF etching from (a).

## 4. Discussion

It is well known that surface nucleation is mainly due to impurity particles whose number is inversely proportional to the degree of surface perfection and cleanliness. Hence, surface crystallization is governed by surface condition of glass. As found in soda-lime-silica and cordierite systems,[15,16] the smoother and presumably the cleaner the surface, the smaller is the crystal density on the surface. According to Muller's survey, the surface nucleation density (N) of differently damaged glass surfaces shows a wide range of $10^{-5}$–$10^{-8}$ $\mu m^{-2}$ for freshly fractured surfaces, $10^{-2}$–$10^{-5}$ $\mu m^{-2}$ for smooth mechanically polished surfaces, and $10^{-2}$–$10^{-3}$ $\mu m^{-2}$ for ground surfaces.[17] There is, however, another theoretical approach to explain surface crystallization with a decrease in the total surface energy or an easier stress relaxation by viscous flow near or at the surface.[18] Schmelzer et al. demonstrated that the elastic strain energy is minimized at the scratches edges, thus favoring nucleation along scratches.[18] The surface crystallization of NdAST was effected by not only the surface condition but also the composition as observed in Table 1. Here it is difficult to say which factor has the most affect on the surface crystal growth because such detailed work is out of the scope of our research. With increasing $TiO_2$ content in NdAS, the slightly lower $T_g$ and $T_x$ (Fig. 1) and the increasing crystal growth rate resulted from increasing the non-bridging oxygen in NdAST glass structure.[5,19] Based on the earlier report, the viscosity of the glasses decreased and the crystal growth rate of the glasses increased with increased content of $TiO_2$.[5] Thus, $TiO_2$ has a positive effect on the growth rate and increases the thickness of the surface crystalline layer compared with the base glass, NdAS. Investigating the controlled crystallization of alkaline earth aluminosilicate glasses, Leger and Bray also noticed that $TiO_2$ enhanced the growth rather than the nucleation rate.[20] It appears that it affects the growth rate by reducing the viscosity of the glasses.

In NdAST glass system, a two-stage heat treatment induced a fine crystal microstructure as an internal crystallization, as shown in Fig. 6. This may be due to the fact that liquid phase separation promotes the nucleation of crystals. Such phenomena took place in

NdAS containing only above 8 wt.% $TiO_2$. [6] There are many similar results on the minimum (threshold) content of $TiO_2$ for volume crystallization as an effective nucleating agent in silicate glass–ceramics.[19,21] In many glass–ceramics, the role of $TiO_2$ during the crystallization of glasses is to form a number of precrystalline events such as enhanced phase separations and/or trace fine crystals.[19] It has been shown in many aluminosilicate glasses ($Li_2O$–$Al_2O_3$–$SiO_2$, CaO–$Al_2O_3$–$SiO_2$, MgO–$Al_2O_3$–$SiO_2$) that the introduction of $TiO_2$ into glasses has a catalyzing effect for heterogeneous nucleation.[22–24] Thus, the action of $TiO_2$ in crystallization of glasses is different in each glass. In this system, $TiO_2$ seems to work to enhance phase separation for internal crystallization and to increase surface crystal growth rate as a network modifier in NdAS glasses. The internal crystallization mechanism in NdAST is suggested as follows: (1) Nucleation occurs in two stages of multiple phase separation. First, large $Nd_2O_3$-rich droplets form and then very small $TiO_2$-rich droplets form in the first droplets (Fig. 8). (2) Crystal growth follows. It is difficult to discuss the precise role of $TiO_2$ in promoting volume nucleation. However, based on the general concept of volume nucleation in silicate glasses [12,13] it could be one of three cases: (1) heterogeneous nucleation on the initial $TiO_2$-rich phase, (2) homogeneous nucleation in the $TiO_2$ rich amorphous phase produced by phase separation or (3) crystal nucleation occurring preferentially at the interface between phases (amorphous droplets), heterogeneously. As shown in the $SiO_2$–$Al_2O_3$–MgO–$TiO_2$ system,[24] the fact that $TiO_2$ can initiate a metastable phase separation as a precursor for the controlled crystallization in the NdAS glass may help to understand the phenomena. Further investigations on nucleation are necessary.

## 5. Conclusions

The crystallization of neodymium aluminosilicate was mainly affected by the content of $TiO_2$ while surface crystallization was also affected by the surface condition of glass. However, internal crystallization induced by phase separation took place in NdAS containing above 8 wt.% $TiO_2$ which had been subjected to a two-stage heat treatment. It was confirmed that $TiO_2$ acts as a nucleating agent in the NdAS system, leading to internal crystallization and that there is a threshold content of $TiO_2$ (8wt.%) required for it to act as an effective nucleating agent in NdAST glasses. The high $TiO_2$ content had a large influence on the crystal growth in surface crystallization and internal crystallization, which produced a glass–ceramic with a microstructure formed of needle type crystals with high aspect ratio.

## Acknowledgements

This work was supported by No.981-1212-036-2 from the Basic Research program of the Korea Science & Engineering Foundation.

## References

1. Shelby, J. E., Rare earths as major component in oxide glass. In *Rare Element in Glasses*, ed. J. E. Shelby. Trans. Tech. Pub, Switzerland, 1994, pp. 1–42.
2. White, J. E. and Day, D. E., Rare earth aluminosilicate glasses for in vivo radiation delivery. In *Rare Element in Glasses*, ed. J. E. Shelby. Trans. Tech. Pub, Switzerland, 1994, pp. 181–208.
3. Kohli, J. T. and Shelby, J. E., Formation of properties of rare earth aluminosilicate glasses. *Physics Chem. Glasses*, 1991, **32**, 67–71.
4. Murakami, Y. and Yamamoto, H., Phase equilibria and properties of glasses in the $Al_2O_3$–$Yb_2O_3$–$SiO_2$ System. *J. Ceram. Soc. Japan*, 1993, **101**, 1071–1075.
5. Baghshahi, S., Brungs, M., Sorrell, C. C. and Kim, H. S., Surface crystallization of rare-earth aluminosilicate glasses. *J. Non-Cryst. Solids*, 2001, **290**, 208–215.
6. Choi, W. H. and Kim, H. S., Phase separation in $Nd_2O_3$–$Al_2O_3$–$SiO_2$-$TiO_2$ glass. *J. Kor. Ceram. Soc.*, 2000, **37**, 1221–1228.
7. Tanabe, S., Hirao, K. and Soga, N., Elastic properties and molar volume of rare-earth alminosilicate glasses. *J. Am. Ceram. Soc.*, 1992, **75**, 503–506.
8. Makishima, A. and Shimohira, T., Alkaline durability of high elastic modulus alumino–silicate glasses containing $Y_2O_3$, $La_2O_3$ and $TiO_2$. *J. Non-Cryst. Solids*, 1980, **38**, 661–666.
9. JCPDS–ICDD, Joint Committee on Powder Diffraction Standards–International Centre for Diffraction Data.
10. CRYSFIRE Program V3.10.
11. Marghussian, V. K. and Niaki, M. H., Effects of composition changes on the crystallisation behaviour and properties of $SiO_2$–$Al_2O_3$–CaO–MgO–($Fe_2O_3$–$Na_2O$–$K_2O$) glass-ceramics. *J. Eur. Ceram. Soc.*, 1995, **15**, 343–348.
12. James, P. F., Kinetics of crystal nucleation in silicate glasses. *J. Non-Cryst. Solids*, 1985, **73**, 517–540.
13. James, P. F., Volume nucleation in silicate glasses. In *Glass and Glass–Ceramics*, ed. M. H. Lewis. Chapman and Hall, London, 1989, pp. 59–105.
14. Kohli, J. T. and Shelby, J. E., Rare-earth aluminogermanate glasses. *J. Am. Ceram. Soc.*, 1991, **74**, 1031–1035.
15. Zanotto, E. D., Experimental studies of surface nucleation and crystallization of glasses. In *Nucleation and Crystallization in Liquids and Glasses*, ed. M. C. Weinberg. American Ceramic Society, Westerville, OH, 1993, pp. 65–74.
16. Granasy, L., Jordery, S., Reaney, I. M., Lee, W. E. and James, P. F., Crystal nucleation in oxide glasses. In *Proceedings of XVIII International Congress on Glass*, ed. M. K. Choudhary. (San Francisco, 5–10 July, USA), 1998.
17. Muller, R., Surface nucleation in cordierite glass. *J. Non-Cryst. Solids*, 1997, **219**, 110–118.
18. Schmelzer, J., Pascora, R., Moller, J. and Gutzow, I. J., Surface-induced devitrification of glasses: the influence of elastic strains. *J. Non-Cryst. Solids*, 1993, **162**, 26–39.
19. McMillan, P. W., *Glass Ceramics*, 2nd edn. Academic Press, London, 1979.
20. Leger, L. and Bray, J., An experimental study of the controlled crystallisation of alkaline earth silico–aluminate glasses. *J. Glass Tech.*, 1966, **7**, 134–142.
21. Duan, R. G., Liang, K. M. and Gu, S. R., Effect of changing

$TiO_2$ content on structure and crystallisation of $CaO–Al_2O_3–SiO_2$ system glasses. *J. Euro. Ceram. Soc.*, 1998, **18**, 1729–1735.

22. Sprengard, R., Fotheringham, U., Pannhorst, W. and Binder, K., Raman-spectroscopic characterisation of nuclei formation in $TiO_2$ nucleated lithium–aluminosilicate glass ceramics. In *Proc. of XVIII International Congress on Glass*, ed. M. K. Choudhary, N. T. Huff and C. H. Drummond, 1998 (CD-ROM).
23. Zou, X., Yamane, Y., Li, J. and Wang, C., Effect of phase separation on nucleation and growth of magnesium–aluminium–titanate crystals in $MgO–Al_2O_3–SiO_2–TiO_2$ glass. *J. Non-Cryst. Solids*, 1988, **112**, 268–271.
24. Varshal, B. G., Knyazher, G. B. and Gelberger, A. M., Liquation in the system $SiO_2–Al_2O_3–MgO–TiO_2$. *Neorganicheskie Materialy*, 1973, **9**, 1809–1815.